



Contents lists available at ScienceDirect



# Catalysis Today

journal homepage: [www.elsevier.com/locate/cattod](http://www.elsevier.com/locate/cattod)

## Methanation of carbon dioxide on Ru/Al<sub>2</sub>O<sub>3</sub>: Catalytic activity and infrared study

Gabriella Garbarino <sup>a,\*</sup>, Daria Bellotti <sup>b</sup>, Elisabetta Finocchio <sup>a</sup>, Loredana Magistri <sup>b</sup>, Guido Busca <sup>a</sup>

<sup>a</sup> Università degli Studi di Genova, Dipartimento di Ingegneria Civile, Chimica e Ambientale (DICCA), P.zza J.F. Kennedy, 1 I-16129 Genova, Italy

<sup>b</sup> Università degli Studi di Genova, Dipartimento di Ingegneria Meccanica, Energetica, Gestionale e dei Trasporti (DIME), Via all'Opera Pia, 15 I-16145 Genova, Italy

### ARTICLE INFO

#### Article history:

Received 3 August 2015

Received in revised form 29 October 2015

Accepted 18 December 2015

Available online xxx

#### Keywords:

Methanation

CO<sub>2</sub>

Ruthenium on alumina

Hydrogenation

Methane

Surface species

### ABSTRACT

3% Ru/Al<sub>2</sub>O<sub>3</sub> catalyst is active in converting CO<sub>2</sub> into methane at atmospheric pressure. At 673 K and above the thermodynamic equilibrium is nearly attained. At 623 K CH<sub>4</sub> yield is above 85%. CO selectivity increases by decreasing reactants partial pressure apparently more than expected by thermodynamics. The reaction order for CO<sub>2</sub> partial pressure is confirmed to be zero, while that related to hydrogen pressure is near 0.38 and activation energy ranges 60–75 kJ/mol. Arrhenius plot demonstrates that only at reduced reactant partial pressure (3% CO<sub>2</sub>) or high contact times, a contribution due to some diffusional limitation is present. IR study shows that the H<sub>2</sub>-reduced catalyst has high-oxidation state Ru oxide species able to oxidize CO to CO<sub>2</sub> at 173–243 K, while after oxidation/reduction cycle the alumina surface acid-basic sites are freed and the catalyst surface contains both extended Ru metal particles and dispersed low valence Ru species. IR studies show that the formation of methane, both from CO and CO<sub>2</sub>, occurs when both surface carbonyl species and surface formate species are observed. Starting from CO<sub>2</sub>, methane is formed already in the low temperature range, i.e., 523–573 K, even when CO is not observed in the gas phase.

© 2016 Elsevier B.V. All rights reserved.

## 1. Introduction

The conversion of CO<sub>2</sub> into methane (methanation)



is one of the possible ways to utilize carbon dioxide thus reducing emissions [1], when hydrogen produced by renewable raw materials or using waste energy is available [2]. To date, commercial catalysts optimized for methanation of feeds primarily composed of carbon dioxide are apparently lacking. Conventional methanation catalysts, optimized to convert feeds containing primarily carbon monoxide, have been mostly tested as CO<sub>2</sub> methanation catalysts and generally found active [3]. Although commercial Ni-based CO methanation catalysts have been found to be active also for CO<sub>2</sub> methanation [4,5] they usually also coproduce significant amounts of CO. Ru based catalysts have been reported since decades to be among the best catalysts for CO<sub>2</sub> methanation [6]. Although Ru/TiO<sub>2</sub> [7], Ru/SiO<sub>2</sub> and Ru/ZSM5 zeolite [8]

have also been reported to be very active, a number of studies show good performances of Ru/Al<sub>2</sub>O<sub>3</sub> catalysts [9–11], essentially better than Ni/Al<sub>2</sub>O<sub>3</sub> catalysts [12]. On the other hand, Ru/Al<sub>2</sub>O<sub>3</sub> catalysts are commercial catalysts for CO methanation for low temperature applications ( $T < 443$  K), such as the Clariant METH-150 catalyst that contains 0.3% ruthenium on alumina [13]. Interestingly, supported ruthenium catalysts are also reported to be the best for CO hydrogenation to higher hydrocarbons, i.e., the Fischer Tropsch process [14,15]. Obviously, for the development of a performant CO<sub>2</sub> methanation process, catalysts producing methane with high selectivity, thus with low CO and higher hydrocarbons coproduction, must be developed.

A point closely related to reaction selectivity is that of reaction mechanism. Until the 1970s, the mechanism of CO methanation was supposed to occur through oxygenated intermediates [6], supported also by more recent spectroscopic studies [16]. However, most recent studies tend to prefer a “via carbide” mechanism, mainly based on “surface science” investigations performed on metal monocrystals. As for the mechanism of CO<sub>2</sub> methanation, an

\* Corresponding author. Fax: +39 103536028.

E-mail address: [Gabriella.Garbarino@unige.it](mailto:Gabriella.Garbarino@unige.it) (G. Garbarino).

additional central point concerns the possible role of CO, produced by the reverse Water Gas Shift reaction (rWGS)



as an intermediate, or/and as a competitor [17,18], the possible intermediacy of carbide species as well as the possible role of the support in adsorbing and activating  $\text{CO}_2$  [19].

To have more information on the surface chemistry of an active Ru/ $\text{Al}_2\text{O}_3$  catalyst and on mechanistic aspects, we deepened our previous studies with further flow reactor experiments and by applying IR spectroscopy methods.

## 2. Experimental

### 2.1. Catalyst characterization

The catalyst used in this study is a 3% (wt%) Ru/ $\gamma$ - $\text{Al}_2\text{O}_3$  commercial catalyst ( $S_{\text{BET}}$  150  $\text{m}^2/\text{g}$ ) from Acta S.p.A. (Crespinia, Pisa, Italy).

IR spectroscopy experiments were performed using a Nicolet Nexus FT instrument. Pressed disks of the pure catalysts powders were treated "in situ" by using an infrared cell connected to a conventional gas manipulation/outgassing ramp in two different ways: by a simply reduction in  $\text{H}_2$  (500 torr) at 673 K for 1 h followed by vacuum treatment at 773 K for 30 min. Alternatively, an oxidation step in air (200 torr) at 673 K for 30 min followed by the same reduction procedure was conducted. The catalyst disk was first submitted to activation and then CO adsorption and reaction experiments were carried out.

CO adsorption was performed at 140 K by the introduction of a known dose of the gas (10 torr) inside the low temperature infrared cell containing the previously activated wafers. IR spectra were recorded during evacuation upon warming at increasing temperatures between 140 K and 673 K.

For the reaction experiments a mixture of  $\text{H}_2$  and  $\text{CO}_2$  (17 torr  $\text{CO}_2$  and 170 torr on IR line and cell) and one of  $\text{H}_2$  and CO (17 torr CO and 170 torr on IR line and cell) were put in contact with the catalyst disk and the reaction was performed step-by-step in-between 523–773 K for ten minutes at each temperature; for each reaction temperature IR spectra of both the gas phase and the catalyst surfaces were acquired.

### 2.2. Catalytic experiments

Catalytic experiments were carried out in a fixed-bed tubular silica glass flow reactor, operating isothermally, loaded with 700 mg of silica glass particles (60–70 mesh sieved) as an inert material mixed with variable amounts of catalyst powder. Different gaseous mixtures of  $\text{CO}_2$  and  $\text{H}_2$  (with excess  $\text{H}_2$ ) diluted with nitrogen were fed, with a total gas flow of 75  $\text{ml}_{\text{NTP}}/\text{min}$ . Temperature was varied step by step in-between 523 K and 773 K (ascending temperature experiment) and back down to 523 K (descending temperature experiment). GHSV calculated as volumetric flow rate (NTP),  $v$  [ $\text{ml}/\text{h}$ ] versus catalyst volume  $V_{\text{cat}}$  [ $\text{ml}$ ] was varied in between 15000 and 55000  $\text{h}^{-1}$ . These values correspond to 5300 and 8000  $\text{h}^{-1}$  if space velocity is calculated taking into account the entire bed volume  $V_{\text{tot}}$ , constituted by silica glass and catalyst powder. Hereinafter we will always refer to the GHSV calculated on the catalyst volume.

Products analysis was performed on line using a Nicolet 6700 FT-IR instrument. Frequencies where  $\text{CO}_2$ ,  $\text{CH}_4$  and CO molecules absorb weakly have been used (2293  $\text{cm}^{-1}$  for  $\text{CO}_2$ , 2100  $\text{cm}^{-1}$  for CO, 1333  $\text{cm}^{-1}$  for  $\text{CH}_4$ , after subtraction of baseline water absorption) with previous calibration using gas mixtures with known concentrations, in order to have quantitative results. Produced water was mostly condensed before the IR cell. From the inlet and

outlet concentrations calculated from the absorbances of CO,  $\text{CO}_2$ ,  $\text{CH}_4$  and the measured inlet and outlet total flows (which allow to take into account the variation of the number of moles during the reaction),  $\text{CO}_2$  conversion ( $X_{\text{CO}_2}$ ), selectivities and yields to products,  $S_i$  and  $Y_i$ , have been calculated [20]. They are defined as:

$$X_{\text{CO}_2} = \frac{F_{\text{CO}_2\text{in}} - F_{\text{CO}_2\text{out}}}{F_{\text{CO}_2\text{in}}} \quad (3);$$

$$S_i = \frac{F_i}{F_{\text{CO}_2\text{in}} - F_{\text{CO}_2\text{out}}} \quad (4);$$

$$Y_i = \frac{F_i}{F_{\text{CO}_2\text{in}}} \quad (5);$$

where  $F_i$  is the molar flow rate of  $i$  (i.e., CO and  $\text{CH}_4$ ), while  $F_{\text{CO}_2}$  is the molar flow rate of  $\text{CO}_2$  and they were all expressed in  $\text{mol}/\text{min}$ .

From the kinetic orders determined in our previous study and from the production rate of  $\text{CH}_4$  we calculated the kinetic constant  $k$  [ $\text{mol}/(\text{min} \times g_{\text{cat}} \times \text{atm}^{0.38})$ ] designing for each test the Arrhenius plot in order to have a better understanding of the controlling regime in the different conditions [12,21].

It should be remarked that, as already reported in our previous work [12], we did not observe any coke formation in our experiments performed at the 8 h timescale. Carbon balance is  $100\% \pm 1\%$  to our calculations and no evidence of coke was obtained from the catalyst weight measure nor from IR, UV-vis, FE-SEM and XRD studies.

## 3. Results and discussion

### 3.1. $\text{CO}_2$ methanation in flow reactor

In Fig. 1, the results of flow reactor  $\text{CO}_2$  methanation experiments (line + symbols) on the 3% Ru/ $\text{Al}_2\text{O}_3$  catalyst are reported and compared with the respective thermodynamic equilibrium for each condition. The three experiments have been performed with the same  $\text{H}_2/\text{CO}_2$  ratio of 5 at 1 atm and the same space velocity (55,000  $\text{h}^{-1}$ ), but with different reactant concentrations. In all cases, no other products than methane and CO were detected. The C balance was always fully fulfilled and no evidence of carbon formation was found using IR, UV-vis, FE-SEM and XRD techniques.

The fresh catalyst is almost not active at 523 K and is only poorly active at 573 K (3%  $\text{CO}_2$  conversion), with a small methane yield slightly increasing with time on stream. In the step performed at 623 K, the catalyst starts to have significant activity that definitely increases with time on stream, due to an activation or "conditioning" step. According to our previous study [12], the catalyst is activated essentially by reduction from a partially cationic to a metallic state. In these conditions, selectivity to methane is 100%, except for the most diluted conditions, where CO is coproduced in small amounts (2–5% yield). At 673 K,  $\text{CO}_2$  conversion is high (from 80% to 84% and from 72% to 79% for 9%  $\text{CO}_2$  and 6%  $\text{CO}_2$  cases, respectively) but still growing with time on stream (Table S1), showing that a "conditioning" effect was still in progress, except again for the most diluted conditions, where the catalyst appears already stable, achieving a  $\text{CO}_2$  conversion of 60% with a methane yield of 47%. At this temperature, CO was also formed together with methane, in particular in the most diluted conditions with a yield of 14%. On the other hand, at the end of the experiments at 673 K the conversion of  $\text{CO}_2$ , the methane yield and selectivity depend clearly on concentration of the reactants, being larger (83–84% for  $\text{CO}_2$  conversion and 82–83% methane yield) when the reactants were more concentrated. By comparison with calculated thermodynamic equilibrium data (Fig. 1 and Table S2 calculated according to [22]),  $\text{CO}_2$  conversion is still markedly lower than the equilibrium one. Thus, the reaction is still under kinetic control, maybe

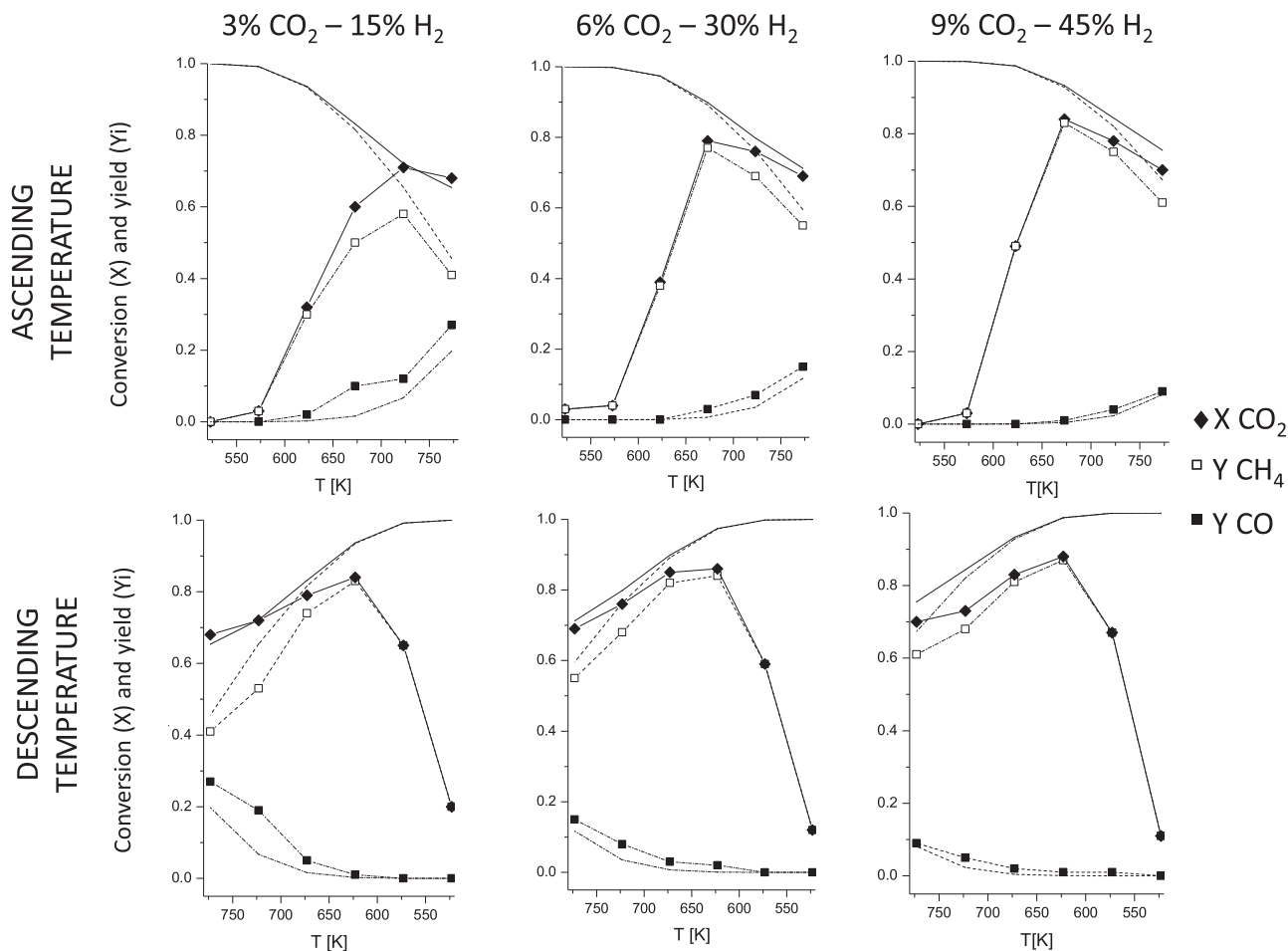


**Fig. 1.** CO<sub>2</sub> hydrogenation results in terms of CO<sub>2</sub> conversion (X) and yields to CO and methane (Y<sub>i</sub>) for different reactants partial pressure at 55,000 h<sup>-1</sup> (82.2 mg catalyst) in the ascending temperature (top) and descending temperature (bottom) experiments (line + symbol). Thermodynamic equilibrium displacement (line) is also reported for each reactant compositions.

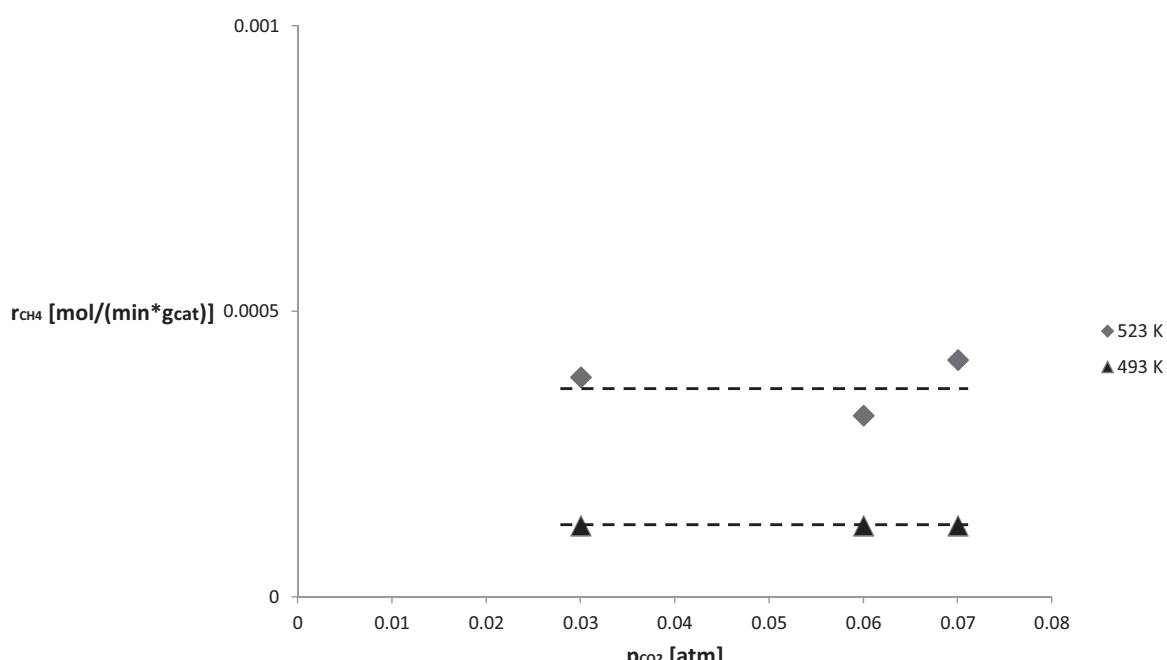


**Fig. 2.** Methane production rate as a function of CO<sub>2</sub> partial pressure ( $P_{CO_2}$ ) and parametric as a function of temperature.

with a minor contribution due to diffusion. However, CO yield is larger, in the experiment at the lowest concentrations, than that expected by thermodynamics.

In the later steps of the experiments (higher temperatures and descending temperatures), with all the three feeds, the catalyst performance was stable with time, showing that "conditioning" was complete and irreversible.

At 723 K, conversion with the most diluted feed was increased with respect to the step at 673 K, while in the other cases conversion decreased. A further decrease of conversion was found at 773 K, in all cases (66–69%  $\text{CO}_2$  conversion). Thermodynamic calculations, whose results are summarized in Fig. 1 and extensively reported in Table S2, reveal that in our conditions we are only slightly below thermodynamic equilibrium at 773 K and 723 K that implies a decrease of  $\text{CO}_2$  conversion by increasing temperature. In agreement with the expected thermodynamically-driven behavior,  $\text{CO}_2$  conversion and methane yield decrease at 773 K, and re-increase in the decreasing temperature steps at 723 K, 673 K and 623 K. We can note that  $\text{CO}_2$  conversion and  $\text{CH}_4$  yield observed at 673 K and 623 K in the decreasing temperature step are markedly higher than those observed, at the same temperature, in the increasing temperature experiment; thus confirming catalyst "conditioning". In the step at 673 K  $\text{CO}_2$  and  $\text{CH}_4$  amounts still agree to be near equilibrium. Also CO is formed and its concentration is definitely higher when the experiment is conducted with lower reactant concentrations. In this case, CO yield at 773 K and 723 K is markedly larger than expected by equilibrium calculation, if the methanation and rWGS reactions are both considered. However, CO yield could be even higher if rWGS only would be taken into account, supposed methanation being hindered kinetically.

By further decreasing temperature to 623 K,  $\text{CO}_2$  conversion further increased (88–84%), as methane yield did, while CO production decreases very much. Here, conversion increases slightly with increasing reactant concentration. However, we are now far from thermodynamic equilibrium, showing that kinetics governs the system at this lower temperature. This is true, even more, at 573 K and 523 K, where catalytic activity is progressively reduced and  $\text{CO}_2$  conversion achieves the lowest value for the descending temperature experiment (11–20%). In spite of this, methane is still formed at 523 K with a 12–20% yield. Thus, the "conditioned" catalyst is still active at 523 K. In this low temperature step the effect of reactant pressure on the conversion and methane yield is really not evident.

In Fig. 2, the effect of  $\text{CO}_2$  partial pressure on reaction rate is shown for experiments performed with the same  $\text{H}_2$  partial pressures, at two different temperatures: we confirm that the reaction order with respect to  $\text{CO}_2$ , determined at 493 K in differential reactor hypothesis [12], essentially zero, remains still valid at 523 K taking into account the experimental error.

In Fig. 3, the Arrhenius plots of the all catalytic tests are reported. The experimental results obtained in the descending temperature experiments, in the temperature range in-between 623 K and 493 K have been considered. Those experiments concern "conditioned" catalysts and refer to conditions were kinetics is determinant. The kinetic constant evaluation ( $k$ , expressed as  $[\text{mol}/(\text{min} \times g_{\text{cat}} \times \text{atm}^{0.38})]$ ) was made dividing the rate of production of methane ( $r_{\text{CH}_4}$ ) by the partial pressure of  $\text{H}_2$  elevated at its reaction order, previously determined (0.38 [12]). A linear behavior can be assumed in all cases at least in the temperature region 493–623 K, except at high contact times, i.e.,  $30000 \text{ h}^{-1}$  (at 623 K) and  $15000 \text{ h}^{-1}$  (at 573 and 623 K). The evident lack of linearity of the plot at high contact times is due to a contribution of diffusional phenomena, since the high conversion, or the approaching of the thermodynamic equilibrium. An analogous situation was found when the lowest partial pressures of the two reactants were used (3%  $\text{CO}_2$ –15%  $\text{H}_2$ ) where again the diffusional effect may be relevant.

From the analysis reported in Fig. 3 the calculated apparent activation energy at low contact times is in the range 60–75 kJ/mol in all cases not far from previous literature data [23]. These values are typical for chemical kinetic regimes, thus assuring that, at least in those conditions, diffusion limitations are negligible.

The trend of CO formation that is higher for the more diluted conditions suggests instead that the reaction orders for CO formation might be even negative, and/or a product inhibition effect can occur for the rWGS reaction producing CO. Alternatively, diffusion limitations for hydrogen availability can occur in these conditions.

### 3.2. IR study of low temperature CO adsorption

In Fig. 4, the spectra associated to CO adsorption at 140 K on the Ru/ $\text{Al}_2\text{O}_3$  catalyst simply reduced in hydrogen are reported. A main band is formed at 140 K centered at  $2151 \text{ cm}^{-1}$ , typically assigned to CO interacting with the surface hydroxyl groups of alumina [24,25]. Additionally a weaker band is observed at  $2025 \text{ cm}^{-1}$ , with a shoulder at  $2000 \text{ cm}^{-1}$ . Upon outgassing at 140 K the band at  $2151 \text{ cm}^{-1}$  quickly disappears confirming its assignment to H-bonded CO and shifting towards higher wavenumbers ( $2159 \text{ cm}^{-1}$ ). Instead, the band found at  $2025$ – $2000 \text{ cm}^{-1}$  does not reduce its intensity until warming to r.t. (room temperature), showing that it is due to strongly bonded CO to zerovalent Ru° [24].

Interestingly, upon warming under dynamic outgassing, a sharp band grows at  $2344 \text{ cm}^{-1}$ , typically due to O-bonded linear  $\text{CO}_2$ . This band starts to be observed at 170 K and raises its maximum intensity at 240 K. By outgassing at higher temperature it decreases rapidly down to disappear at 270 K, due to  $\text{CO}_2$  desorption. The weak band at  $2278 \text{ cm}^{-1}$  is due to the corresponding  $^{13}\text{CO}_2$  adsorbed species, according to the natural abundance of C isotopes. This shows that the sample surface, in spite of the reducing pre-treatment, still retains oxidation functionality, oxidizing CO to  $\text{CO}_2$ . This functionality is certainly associated to un-reduced  $\text{Ru}^{x+}$ , whose charge is balanced by anions such as active oxygen species. These ruthenium oxide species reacts with CO reducing itself. Below 170 K this reaction is kinetically hindered and a band characterizing the interaction of CO with such un-reduced Ru species should be observed. This band is actually superimposed by that of CO interacting with OH groups. In fact, a number of unresolved components can be found on this band, whose maximum shifts to higher frequencies upon outgassing and warming, but that shows visible shoulders at  $2165 \text{ cm}^{-1}$  at the higher temperature and at  $2135 \text{ cm}^{-1}$  at the lowest one. Indeed, the interaction of CO with  $\text{RuO}_2$  (110) monocrystals has been studied by Ertl and coworkers using surface techniques, showing a CO stretching band at  $2115 \text{ cm}^{-1}$ , and the easy oxidation of CO to  $\text{CO}_2$  above 300 K [26]. On the other hand, CO adsorbed on  $\text{RuO}_2/\text{SiO}_2$  has been reported to adsorb at  $2125 \text{ cm}^{-1}$  [27]. These data confirm that simple reduction in hydrogen is not sufficient to fully reduce the catalyst and activate it, as discussed previously [12].

In Fig. 5 the spectra relative to a similar experiment performed on preoxidized and later reduced Ru/ $\text{Al}_2\text{O}_3$  catalyst are reported. At 140 K, the band due to CO interacting with OH groups is still the most intense, but is now found at  $2160 \text{ cm}^{-1}$ . However, two other strong adsorptions are observed. A band at  $2192 \text{ cm}^{-1}$ , decreasing and shifting up progressively upon warming down to  $2207 \text{ cm}^{-1}$ , can be assigned to CO interacting with  $\text{Al}^{3+}$  cations. These species disappear after outgassing at  $T > 240 \text{ K}$ .

A strong and quite broad band, centered at  $2037 \text{ cm}^{-1}$ , is also observed. Its intensity decreases and its position is shifted towards lower frequency during sample outgassing upon warming. In particular, this band, presents its maximum at  $2037 \text{ cm}^{-1}$  upon outgassing at 140 K and then is centered near  $1990 \text{ cm}^{-1}$  upon outgassing at 423 K. Above 423 K the observed features

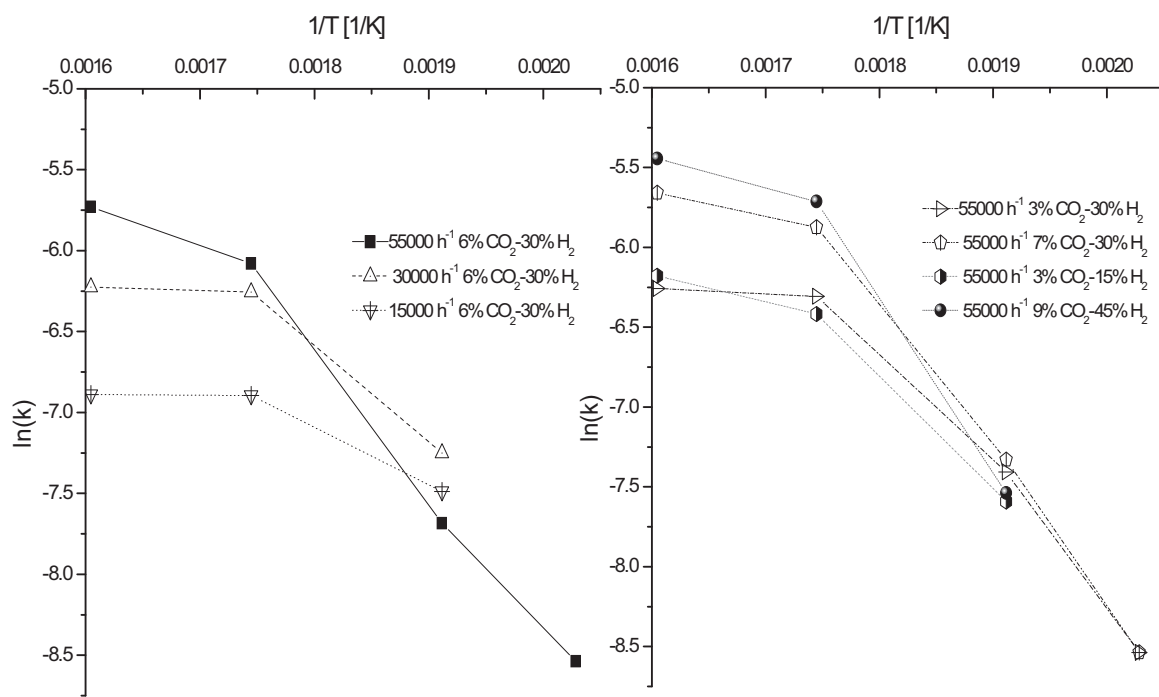


**Fig. 3.** Arrhenius's plot ( $k$  [mol/(min ×  $g_{\text{cat}}$  × atm<sup>0.38</sup>)] of all the catalytic tests performed with experimental points (symbols) as a function of  $1/T$ .

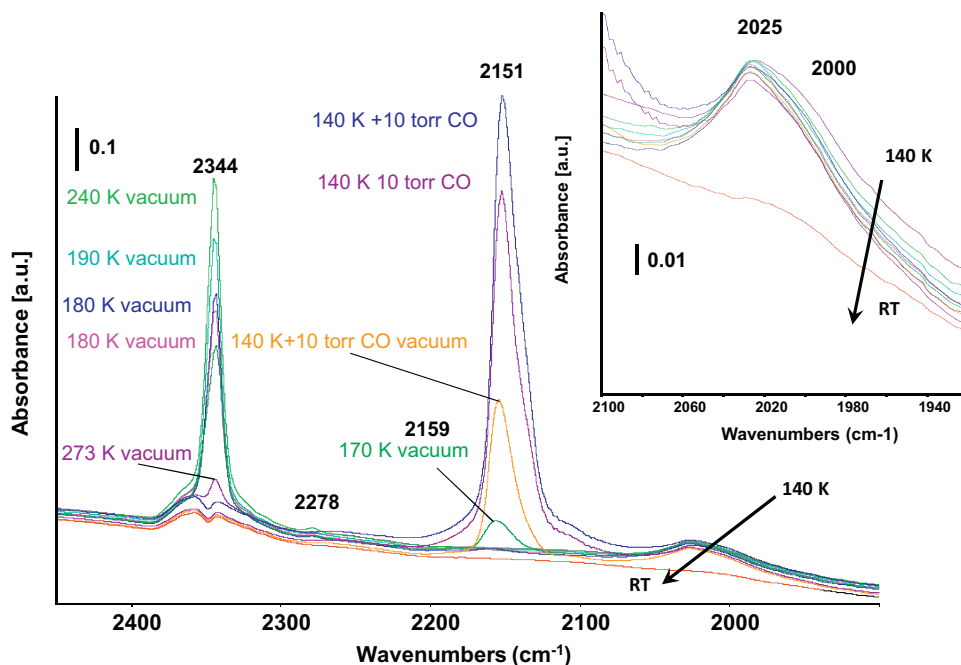


**Fig. 4.** CO adsorption at liquid nitrogen temperature on the prerduced sample. IR surface spectra at 140 K, in contact with 10 torr of CO and upon outgassing until RT. Inset: magnification of the low frequency region.

further decrease in intensity without clear shifting. They are observed at 2142, 2075, 2004 and 1960 cm<sup>-1</sup> approximately.

The band shifting from 2037 cm<sup>-1</sup> down to ca 1990 cm<sup>-1</sup> is clearly due to CO adsorbed on extended Ru metal particles, shifting down upon decreasing coverage due to the well-known coupling effects depending on the coverage. The range of the frequency does not allow to distinguish between flat and stepped faces such as Ru (001) [28], Ru (01̄20) [29] and Ru (109) [30]. The non-shifting bands at 2142, 2075, 2004 and 1960 cm<sup>-1</sup> instead should be assigned to CO interacting with isolated or clustered Ru° or Ru<sup>δ+</sup> centers

[24]. A triplet similar to our at 2142, 2075 and 2004 cm<sup>-1</sup> has been observed by Darenbourg and Ovalles [31] on a RuCl<sub>3</sub>/Al<sub>2</sub>O<sub>3</sub> catalyst and assigned to Ru polycarbonyls, and by Elmasides et al. [32] on a 0.5% Ru/Al<sub>2</sub>O<sub>3</sub> sample after reduction in hydrogen and has been assigned to polycarbonyl species on well dispersed ionic Ru. A similar triplet was also observed by Chin et al. [33] on 1% Ru/Al<sub>2</sub>O<sub>3</sub> after prerduction in hydrogen by in copresence of CO with oxygen. These authors assigned the triplet to the superimposition of two doublets due to dicarbonyl species on ionic and zerovalent Ru. The residual band at 1960 cm<sup>-1</sup> can be due to bridging CO on Ru

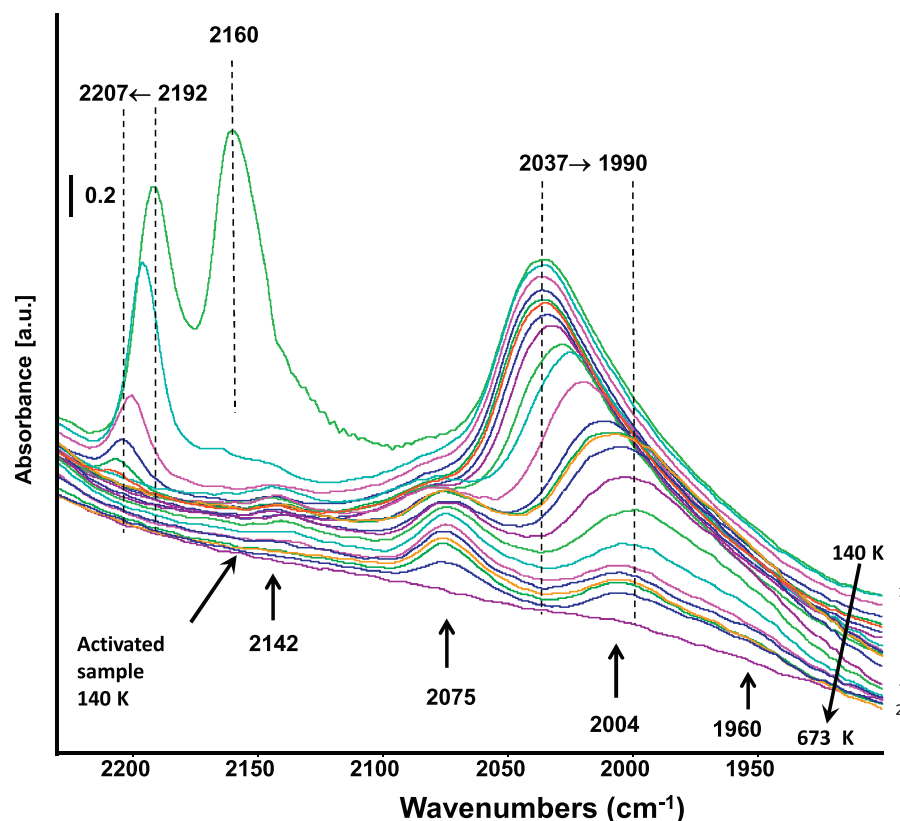


**Fig. 5.** CO adsorption at liquid nitrogen temperature on the preoxidized and reduced sample. IR surface spectra at 140 K (spectrum 24), in contact with 10 torr of CO (spectrum 1), upon outgassing in-between 140–298 K (spectra 2–15) and upon heating 673 K (spectra 16–23).

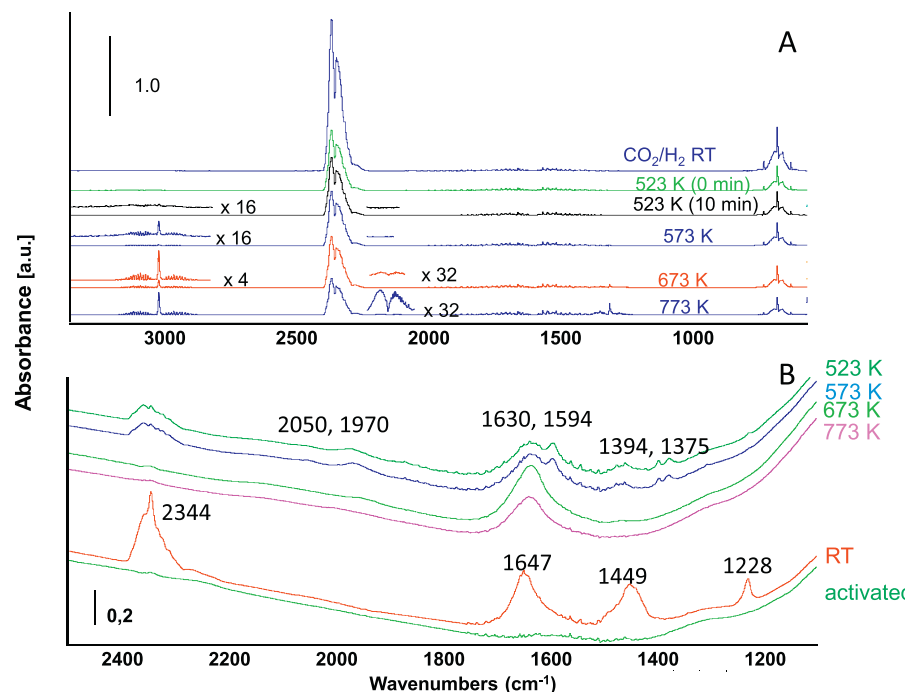


**Fig. 6.**  $\text{CO}_2 + \text{H}_2$  reactivity in the IR cell (total pressure 170 torr,  $\text{CO}_2$  17 torr). Gas phase (A) and surface adsorbed species (B) after 10 min at the reaction temperature.

clusters. Although a more precise assignment of these bands cannot be proposed on the basis of the reported data, it seems very likely that the reduced Ru catalyst contains both extended metal particles and likely more than one family of small clusters or isolated Ru in the zerovalent or ionic state. In any case, the hydrogen

reduced catalyst lost its ability to oxidize CO, highly oxidized Ru species (likely  $\text{Ru}^{4+}$ ) having been reduced.

The oxidizing and reducing pretreatments give rise to different ruthenium species on the surface than those observed by pure reduction in  $\text{H}_2$ . This is an useful information in connection to con-

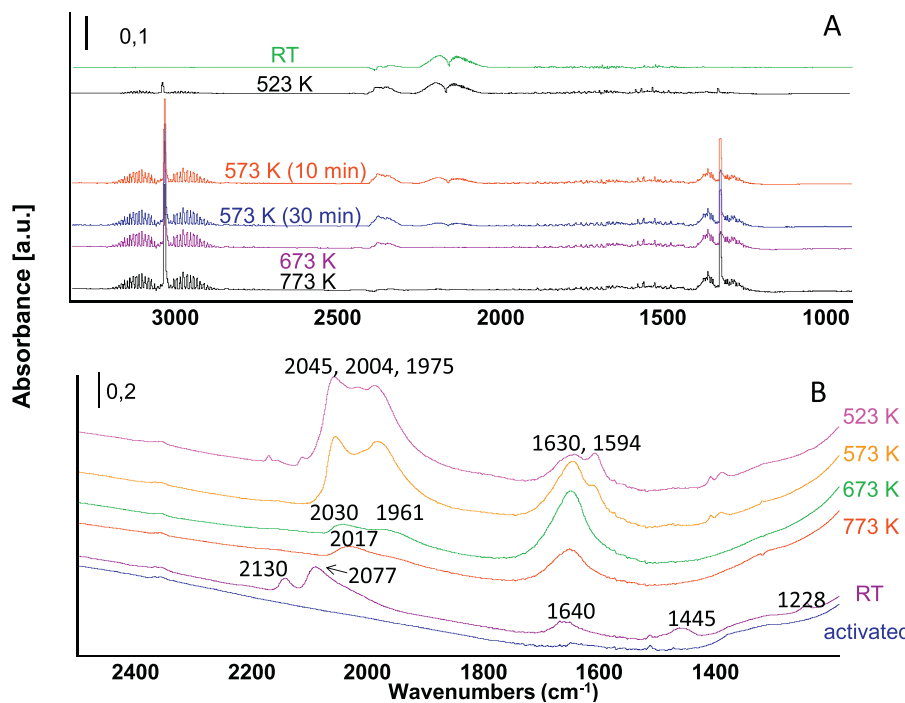


**Fig. 7.** CO + H<sub>2</sub> reactivity in the IR cell (total pressure 170 torr, CO 17 torr). Gas phase (A) surface adsorbed species (B) after 10 min at the reaction temperature.

ditioning and regeneration and to the exposure of the catalyst to different atmospsheres as well. This behavior is likely connected not only to oxidation/reduction of Ru species but also to the possible removal of chlorine, residual from catalyst preparation, as reported previously [12].

The difference between the spectra reported in Figs. 4 and 5 indicates that after impregnation, and even after reduction in hydrogen, highly charged cationic Ru species interact on alumina surface defects where also Lewis acidic Al<sup>3+</sup> are located. This interaction inhibits or kills the Al<sup>3+</sup> Lewis acid sites, which interact with CO (band above 2180 cm<sup>-1</sup> [34]) and not observed. Small amounts of isolated or clustered Ru° are also observed probably located on the main faces (CO bands at 2025–2000 cm<sup>-1</sup>). The further treatment of ruthenium oxidation and reduction frees Lewis acidic Al<sup>3+</sup> centers (CO bands at 2192–2207 cm<sup>-1</sup>) now evident, corresponding to partial agglomeration of Ru species, producing particles, clusters and isolated Ru atoms.

### 3.3. IR study of CO<sub>2</sub> hydrogenation

In Fig. 6A the gas phase spectra recorded upon contacting of the prerduced catalyst disk with CO<sub>2</sub> + H<sub>2</sub> mixture in the IR cell are reported. The reaction is very slow at 523 K producing very small amounts of methane (rotovibrational bands with maxima at 3016 cm<sup>-1</sup> and 1305 cm<sup>-1</sup>, asymmetric stretching and deformation respectively) and only a small decrease of the band of CO<sub>2</sub> (rotovibrational bands with minima at 3716, 3613 cm<sup>-1</sup>, combination modes, and 2349 cm<sup>-1</sup>, asymmetric stretching, and with maximum at 669 cm<sup>-1</sup>, deformation mode). At 573 K and 673 K the reaction is faster than that achieved at 523 K (lowest temperature used in the experiments), resulting in the detection of stronger methane signals. Interestingly, only methane is found in the gas phase at 523 K and 573 K, while very small amounts of CO (rotovibrational band with minimum at 2140 cm<sup>-1</sup>) are also observed at 673 K and above. The spectra of the surface species recorded upon the experiment are reported in Fig. 6B. Adsorption of the catalyst of the CO<sub>2</sub> + H<sub>2</sub> mixture at r.t. (Room Temperature, i.e., 298 K) produces O-bonded linearly adsorbed

CO<sub>2</sub> (2344 cm<sup>-1</sup>, OCO asymmetric stretching) and bicarbonate species (1647 cm<sup>-1</sup>, 1449 cm<sup>-1</sup>, asymmetric and symmetric COO stretching, 1228 cm<sup>-1</sup>, OH deformation) which is associated to the weak basicity of alumina support [25]. The position of these bands is the same observed when these species are formed on pure alumina, thus indicating that they are interacting with alumina more than with ruthenium species. On the other side, the spectra of exposed hydroxyl groups on this catalyst are consistent with those reported for typical γ-aluminas, maybe slightly modified by ruthenium deposition [34]. At 523 K, bands assigned to formate species (1594 cm<sup>-1</sup> asymmetric COO-stretching, 1394 cm<sup>-1</sup> CH deformation, 1375 cm<sup>-1</sup> COO-symmetric stretching) are also observed. The position of these bands is the same observed when these species are formed on pure alumina, thus indicating that they are not interacting with ruthenium. Together, weak bands at 2050 and 1970 cm<sup>-1</sup> are observed. These features should be due to small amounts of strongly adsorbed CO species. They look similar to the doublets typical of Ru dicarbonyl species as such and adsorbed on alumina [31]. The band at 1630 cm<sup>-1</sup>, associated also to strong absorption in the 3600–3200 cm<sup>-1</sup> region, is due to adsorbed water.

This experiment shows that CH<sub>4</sub> gas is formed before (at lower temperature, i.e. 523 K) than CO gas (673 K), thus suggesting that CO gas may be not an intermediate in CO<sub>2</sub> methanation. However, also the amount of adsorbed CO is very small. The data also suggest that the way bicarbonate-formate-methane is a possible way to CO<sub>2</sub> methanation on Ru catalyst. The formation of methoxy groups is not evident nor the formation of CH<sub>x</sub> species can be observed by looking at the CH stretching region.

### 3.4. IR study of CO hydrogenation.

In Fig. 7A the gas phase spectra recorded upon contacting of the prerduced catalyst with CO + H<sub>2</sub> mixture. The reaction already occurs at 523 K producing significant amounts of methane and water. The reaction is faster at 673 K and above. No other hydrocarbons are found, unlike previous experiments performed in similar conditions on Ru/TiO<sub>2</sub> experiments [15,35]. The spectra of the surface species recorded upon the exper-

iment are reported in Fig. 7B. Adsorption of the catalyst of the CO+H<sub>2</sub> mixture at RT produces carbonyl species absorbing at 2130 and 2077 cm<sup>-1</sup>, and bicarbonate species (1647 cm<sup>-1</sup>, 1449 cm<sup>-1</sup>, asymmetric and symmetric COO stretching, 1228 cm<sup>-1</sup>, OH deformation). According to the above study, the doublet at 2130 and 2077 cm<sup>-1</sup> could be assigned to dicarbonyls on ionic Ru. At 523 K, formate species (1594 cm<sup>-1</sup> asymmetric COO stretching, 1394 cm<sup>-1</sup> CH deformation, 1375 cm<sup>-1</sup> COO symmetric stretching) are also observed, together with water (1630 cm<sup>-1</sup>), and strong bands due to carbonyl species (2045, 2004, 1975 cm<sup>-1</sup>). This spectrum suggests that at this temperature Ru is reduced forming metal particles and clusters of zerovalent Ru. At 673 K formate species disappeared, while weak bands of carbonyl species are observed (2030, 1961 cm<sup>-1</sup>). The spectra show that carbonyl species are likely intermediate in CO methanation, although formate species may also play a role. Again, in contrast to previous experiments performed with Ru/TiO<sub>2</sub> catalysts [15], the formation of adsorbed CH<sub>x</sub> species cannot be observed by looking at the CH stretching region. This suggests indeed that evident CH species are precursors for higher hydrocarbons (Fischer Tropsch synthesis) more than intermediates in methanation.

#### 4. Conclusion

The main conclusions can be summarized as follows.

The 3% Ru/Al<sub>2</sub>O<sub>3</sub> catalyst is active in converting CO<sub>2</sub> into methane at atmospheric pressure. At 673 K the performances observed approach closely the thermodynamic equilibrium. At 623 K the maximum CO<sub>2</sub> conversion and CH<sub>4</sub> yield are obtained both in the range above 85%. In the kinetically controlled regime ( $T < 623$  K, with the exceptions discussed in the text), the reaction order for CO<sub>2</sub> conversion with respect to CO<sub>2</sub> pressure is zero, while that related to hydrogen pressure is near 0.38. The activation energy ranges 60–75 kJ/mol. The selectivity to CO increases by decreases reactants partial pressure apparently more than expected by thermodynamics, may be due to some diffusion limitation.

Even after reduction in hydrogen, the catalyst shows high-oxidation state Ru oxide species able to oxidize CO to CO<sub>2</sub> at 173–243 K. These species are dispersed on alumina crystal defects (edges, corners, structural defects) thus perturbing the alumina strongest surface acid-base sites.

After oxidation/reduction cycles, the alumina surface acid-base sites are freed, and the catalyst surface contains both extended Ru particles and dispersed low valence Ru species. CO adsorption produces terminal carbonyls on extended faces and polycarbonyls on dispersed Ru species, and CO on alumina Lewis sites as well. CO<sub>2</sub> adsorbs essentially on the alumina support in the form of bicarbonate species as well as in a molecular species.

IR studies show that the formation of methane, both from CO and CO<sub>2</sub>, occurs when both surface carbonyl species and surface formate species are observed on the surface. Starting from CO<sub>2</sub>, methane is formed already in the low temperature range, i.e., 523–573 K, even when CO is not observed in the gas phase. This suggests that gas-phase CO might be not an intermediate in CO<sub>2</sub> methanation.

#### Appendix A. Supplementary data

Supplementary data associated with this article can be found, in the online version, at <http://dx.doi.org/10.1016/j.cattod.2015.12.010>.

#### References

- [1] G. Centi, S. Perathoner, *Catal. Today* 148 (2009) 191–205.
- [2] S.K. Hoekman, A. Broch, C. Robbins, R. Purcell, *Int. J. Greenhouse Gas Control* 4 (2010) 44–50.
- [3] W. Wang, J. Gong, *Front. Chem. Sci. Eng.* 5 (2011) 2–10.
- [4] S. Abelló, C. Berueco, D. Montañé, *Fuel* 113 (2013) 598–609.
- [5] G. Garbarino, P. Riani, L. Magistri, G. Busca, *Int. J. Hydr. En.* 39 (2014) 11557–11565.
- [6] G.A. Mill, F.W. Steffgen, *Chem. Rev.* 8 (1973) 159.
- [7] M. Matwood, R. Doepper, A. Renken, *Appl. Catal. A* 151 (1997) 223–246.
- [8] S. Scirè, C. Crisafulli, R. Maggiore, S. Minicò, S. Galvagno, *Catal. Lett.* 51 (1998) 41–45.
- [9] D.J. Dahrenbourg, C. Ovalles, *Inorg. Chem.* 25 (1986) 1603–1609.
- [10] J.H. Kwak, L. Kovarik, L. Szanyi, *ACS Catal.* 3 (2013) 2449–2455.
- [11] C. Janke, M.S. Duyar, M. Hoskins, R. Farrauto, *Appl. Catal. B* 152 (2014) 184–191.
- [12] G. Garbarino, D. Bellotti, P. Riani, L. Magistri, G. Busca, *Int. J. Hydrogen Energy* 40 (2015) 9171–9182.
- [13] <http://www.catalysts.clariant.com/bu/Catalysis/internet.nsf/023cfbb98594ad5bc12564e400555162/4cf7847d693c1f0c1257ad0002d2c04?OpenDocument>.
- [14] G.P. van der Laan, A.A.C.M. Beenackers, *Catal. Rev. Sci. Eng.* 41 (1999) 255–318.
- [15] J.M. González Carballo, E. Finocchio, S. García, S. Rojas, M. Ojeda, G. Busca, J.L. García Fierro, *Catal. Sci. Technol.* 1 (2011) 1013–1023.
- [16] V. Sanchez-Escribano, M.A. Larrubia Vargas, E. Finocchio, G. Busca, *Appl. Catal. A* 316 (2007) 68–74.
- [17] K. Yaccato, R. Corhart, A. Hagemeyer, A. Lesik, P. Strasser, A.F. Volpe, H. Turner, H. Weinberg, R.K. Grasselli, C. Brooks, *Appl. Catal. A* 296 (2005) 30–48.
- [18] A.M. Abdel-Mageed, S. Eckle, H.G. Anfang, R.J. Behm, *J. Catal.* 298 (2013) 148–160.
- [19] F. Ussa Aldana, K. Ocampo, B. Kobl, F. Louis, M. Thibault-Starzyk, P. Daturi, S. Bazin, A.C. Thomas, *Catal. Today* 215 (2013) 201–207.
- [20] O. Levenspiel, *Chemical Reaction Engineering*, 3rd, Wiley New York, 1999, pp. 87.
- [21] H.S. Fogler, *Elements of Chemical Reaction Engineering*, fourth, Pearson Education International, New Jersey, 2006.
- [22] R.D. Reid, J.M. Prausnitz, B.E. Poling, *The Properties of Gases and Liquids*, 4th, McGraw-Hill, New York, 1986.
- [23] M.R. Praire, A. Renken, J.G. Highfield, K. Ravindranathan Thampi, M. Grätzel, *J. Catal.* 129 (1991) 130–144.
- [24] G. Hadjiivanov, Vayssiolov, *Adv. Catal.* 47 (2002) 307–511.
- [25] T. Montanari, L. Castoldi, L. Lietti, G. Busca, *Appl. Catal. A* 400 (2011) 61–69.
- [26] J. Wang, C.Y. Fan, K. Jacobi, G. Ertl, *Surf. Sci.* 481 (2001) 113–118.
- [27] M. Sorlino, G. Busca, *Appl. Surf. Sci.* 18 (1984) 268–272.
- [28] H. Pfür, D. Menzel, F.M. Hoffmann, A. Ortega, A.M. Bradshaw, *Surf. Sci.* 93 (1980) 431.
- [29] J. Wang, Y. Wang, K. Jacobi, *Surf. Sci.* 488 (2001) 83–89.
- [30] T. Zubkov, G.A. Morgan Jr., J.T. Yates Jr., O. Kuhlert, M. Lisowski, R. Schillinger, D. Fick, H.J. Jansch, *Surf. Sci.* 526 (2003) 57–71.
- [31] D.D. Dahrenbourg, C. Ovalles, *Inorg. Chem.* 25 (1986) 1603–1609.
- [32] C. Elmasides, D.I. Kondarides, W. Grunert, X.E. Verykios, *J. Phys. Chem. B* 103 (1999) 5227–5239.
- [33] S.Y. Chin, C.T. Williams, M.D. Amiridis, *J. Phys. Chem. B* 110 (2006) 871–882.
- [34] G. Busca, *Adv. Catal.* 57 (2014) 319–404.
- [35] J.M. González Carballo, E. Finocchio, S. García-Rodríguez, M. Ojeda, J.L.G. Fierro, G. Busca, S. Rojas, *Catal. Today* 214 (2013).